



# A unified framework for perceived magnitude and discriminability of sensory stimuli

Jingyang Zhou<sup>a,b,1</sup> , Lyndon R. Duong<sup>b</sup> , and Eero P. Simoncelli<sup>a,b,c,1</sup>

Edited by Roberta Klatzky, Carnegie Mellon University, Pittsburgh, PA; received July 18, 2023; accepted April 25, 2024

The perception of sensory attributes is often quantified through measurements of sensitivity (the ability to detect small stimulus changes), as well as through direct judgments of appearance or intensity. Despite their ubiquity, the relationship between these two measurements remains controversial and unresolved. Here, we propose a framework in which they arise from different aspects of a common representation. Specifically, we assume that judgments of stimulus intensity (e.g., as measured through rating scales) reflect the mean value of an internal representation, and sensitivity reflects a combination of mean value and noise properties, as quantified by the statistical measure of Fisher information. Unique identification of these internal representation properties can be achieved by combining measurements of sensitivity and judgments of intensity. As a central example, we show that Weber's law of perceptual sensitivity can coexist with Stevens' power-law scaling of intensity ratings (for all exponents), when the noise amplitude increases in proportion to the representational mean. We then extend this result beyond the Weber's law range by incorporating a more general and physiology-inspired form of noise and show that the combination of noise properties and sensitivity measurements accurately predicts intensity ratings across a variety of sensory modalities and attributes. Our framework unifies two primary perceptual measurements—thresholds for sensitivity and rating scales for intensity—and provides a neural interpretation for the underlying representation.

Fisher information | Weber's law | Stevens' power law | Fechner's law | stochastic representation

On a blistering summer's day, we sense the heat. And just as readily, we sense the cooling relief from the onset of a soft breeze. Our ability to gauge the absolute strength of sensations, as well as our sensitivity to changes in their strength, are ubiquitous and automatic. These two judgments have also shaped the foundations of our knowledge of sensory perception.

Perceptual capabilities arise from our internal representations of sensory inputs. Measurements of sensitivity to changes in these inputs have sculpted our understanding of sensory representations across different domains. For example, in the late 1800s, Fechner proposed that sensitivity to a small change in a stimulus is proportional to the resulting change in the internal representation of that stimulus (1). By the 1950s, signal detection theory was formulated to describe this in terms of stochastic internal representations (e.g., refs. 2 and 3), generalizing beyond Fechner's implicit assumption that stimuli are represented deterministically. In addition to sensitivity to stimulus changes, humans and animals can also make absolute judgments of stimulus intensities (4–8). But the experimental methods by which this can be quantified are more controversial (9, 10), and the measurements have proven difficult to relate to sensitivity measurements (11–14).

Consider the well-known example of Weber's law, which states that perceptual thresholds for reliable stimulus discrimination scale proportionally with stimulus intensity (equivalently, sensitivity scales inversely with intensity). Weber's law holds for an impressive variety of stimulus attributes. Fechner's broadly accepted explanation is that sensitivity reflects the change in an internal representation that arises from a small change in the stimulus (specifically, it reflects the derivative of the function that maps stimulus intensity to representation). For Weber's law, this implies a logarithmic internal representation. The search for physiological evidence supporting Fechner's proposal has been ongoing for more than a century, but remains inconclusive (e.g., refs. 4 and 15). In the 1950s, Stevens and others found that human ratings of perceived intensity of a variety of sensory attributes (proposed as an alternative measure of internal representation) follow a power law, with exponents ranging from strongly compressive to strongly expansive (16, 17). Stevens presented this as a direct refutation of Fechner's logarithmic hypothesis (11), but offered no means of reconciling the two. Subsequent explanations have generally proposed either that intensity and sensitivity judgments arise from different perceptual

## Significance

Measurements of sensitivity to stimulus changes and stimulus appearance (intensity) are ubiquitous in the study of perception. However, the relationship between these two seemingly disparate measurements remains unclear. Proposals for unification have been made for over 60 y, but they generally lack support from perceptual or physiological measurements. Here, we provide a framework that offers a unified interpretation of perceptual sensitivity and intensity measurements, and we demonstrate its consistency with experimental measurements across multiple perceptual domains.

Author affiliations: <sup>a</sup>Center for Computational Neuroscience, Flatiron Institute, Simons Foundation, New York, NY 10010; <sup>b</sup>Center for Neural Science, New York University, New York, NY 10003; and <sup>c</sup>Courant Institute of Mathematical Sciences, New York University, New York, NY 10003

Author contributions: J.Z., L.R.D., and E.P.S. designed research; J.Z. and E.P.S. performed research; J.Z. and E.P.S. contributed new reagents/analytic tools; J.Z. analyzed data; and J.Z., L.R.D., and E.P.S. wrote the paper.

The authors declare no competing interest.

This article is a PNAS Direct Submission.

Copyright © 2024 the Author(s). Published by PNAS. This open access article is distributed under Creative Commons Attribution-NonCommercial-NoDerivatives License 4.0 (CC BY-NC-ND).

<sup>1</sup>To whom correspondence may be addressed. Email: jyzhou@flatironinstitute.org or eero.simoncelli@nyu.edu.

This article contains supporting information online at <https://www.pnas.org/lookup/suppl/doi:10.1073/pnas.2312293121/-DCSupplemental>.

Published June 10, 2024.

representations (18–21) or that the two perceptual tasks involve different nonlinear cognitive transformations (22, 23).

Here, we generalize Fechner's solution, developing a framework to interpret and unify perceptual sensitivity and intensity judgments of continuous sensory attributes. Specifically, we use a simplified form of Fisher information (FI) to generalize classical signal detection theory, and use this to quantify the relationship between perceptual sensitivity and the noisy internal representation. We show that a family of internal representations with markedly different noise properties are all consistent with Weber's law, but only one form is also consistent with power law intensity percepts. Finally, by incorporating a noise model that is compatible with physiology, we demonstrate that the framework can unify sensitivity and intensity measurements beyond the regime over which Weber's law and Stevens' power law hold, and for a diverse set of sensory attributes.

## Results

What is the relationship between perceptual sensitivity, and the internal representations from which it arises? Intuitively, a change in stimulus value (e.g., contrast of an image) leads to a change in internal response. When the change in internal response is larger than the noise variability in that response, we are able to detect the stimulus change. This conceptualization, based on Fechner's original proposals (1) and formalized in the development of signal detection theory in the middle of the 20th century, has provided a successful quantitative framework to analyze and interpret perceptual data (2, 3, 24). Despite this success, signal detection theory formulations are usually not explicit about the transformation of stimuli to internal representations, and most examples in the literature assume that internal responses are corrupted by noise that is additive, independent, and Gaussian.

A more explicit relationship between sensitivity and internal representation may be expressed using a statistical tool known as FI. Specifically, the noisy internal responses ( $r$ ) to a stimulus ( $s$ ) are described by a conditional probability  $p(r|s)$ , and FI is defined in terms of a second-order expansion of this probability:  $F(s) = \mathbb{E}[(\partial \log p(r|s)/\partial s)^2]$ . This quantity specifies the precision with which the stimulus can be recovered from the noisy responses, and  $\sqrt{F(s)}$  provides a measure of sensitivity to stimulus changes (Materials and Methods). FI is quite general: It can be used with any continuous stimulus attribute, and any type of response distribution (including multimodal, discrete, and multidimensional responses), although only a subset of cases yield an analytic closed-form expression. In engineering, it is used to compute the minimum achievable error in recovering signals from noisy measurements (known as the “Cramér–Rao bound”). In perceptual neuroscience, it has been used to describe the precision of sensory attributes represented by noisy neural responses (25–28), as a bound on discrimination thresholds (29–31) and to synthesize optimally discriminable stimuli (32).

**Interpreting Weber's Law using FI.** Typically, FI is used to characterize decoding errors based on the specification of an encoder. Here, we are interested in the reverse: we want to constrain properties of an internal representation (an encoder) based on external measurements of perceptual sensitivity (decoder errors). Consider Weber's law, in which perceptual sensitivity of a stimulus attribute is inversely proportional to the value of the attribute. If we assume observers achieve the bound expressed by the FI, this implies that  $\sqrt{F(s)} \propto 1/s$ . What internal representation,  $p(r|s)$ , underlies this observation? The

answer is not unique. Although the complete family of solutions is not readily expressed, we can deduce and verify a set of three illustrative examples (Fig. 1).

First, Weber's law can arise from a nonlinear internal representational mean  $\mu(s)$  (often referred to as a “transducer function”). If we assume that  $\mu(s)$  is contaminated by additive Gaussian noise with variance  $\sigma^2$  (3, 33, 34):  $p(r|s) \sim \mathcal{N}[\mu(s), \sigma]$ , then  $\sqrt{F(s)} = |\mu'(s)|/\sigma$  (Materials and Methods). Thus, sensitivity to small stimulus perturbations is proportional to the derivative of the representational mean. Notice that this is a differential version of the standard measure of “d-prime” in signal detection theory, which is used to quantify discriminability of two discrete

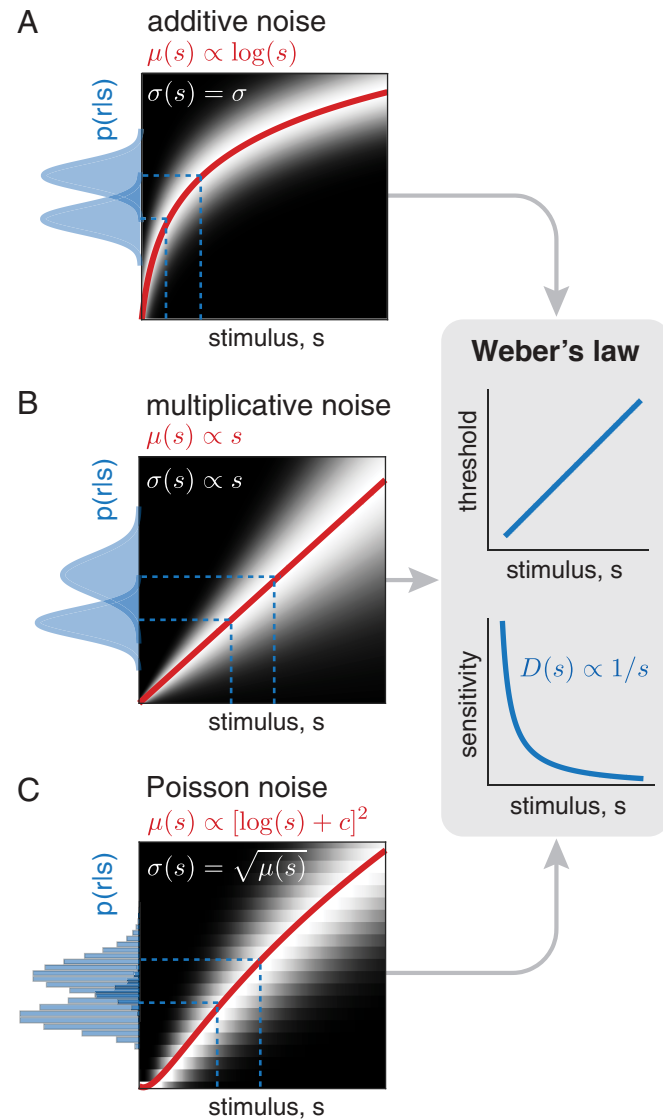


**Fig. 1.** Three different internal representations, each consistent with Weber's law. Each panel on the Left shows a stimulus-conditional response distribution,  $p(r|s)$  (grayscale image, brightness proportional to conditional probability), the mean response  $\mu(s)$  (red line), and response distributions for two example stimuli (blue, plotted vertically). (A) Mean response proportional to  $\log(s)$ , contaminated with additive Gaussian noise, with constant SD,  $\sigma(s) = \sigma$ . (B) Mean response proportional to  $s$ , with “multiplicative” Gaussian noise ( $\sigma(s)$  is also proportional to  $s$ ). (C) Mean response proportional to  $[\log(s) + c]^2$  with Poisson (integer) response distribution, for which  $\sigma(s) = \sqrt{\mu(s)}$ . The panel on the Right indicates the perceptual discrimination threshold (Top) and the sensitivity (Bottom) that arise from the calculation of FI, which are identical for all three representations.

stimuli (*SI Appendix*). Under these conditions, sensitivity follows Weber's law if the transducer is  $\mu(s) \propto \log(s) + c$ , with  $c$  an arbitrary constant (Fig. 1A illustrates a case when  $c = 0$ , also see *Materials and Methods*). This logarithmic model of internal representation, due to Fechner (1, 5), is the most well-known explanation of Weber's law.

Alternatively, a number of authors proposed that Weber's law arises from representations in which noise amplitude grows in proportion to stimulus strength (sometimes called "multiplicative noise") (3, 35–40). Suppose representational mean  $\mu(s)$  is proportional to stimulus strength ( $s$ ), and is contaminated by Gaussian noise with standard deviation (SD) also proportional to  $s$ :  $p(r|s) \sim \mathcal{N}[s, s^2]$ . The square root of FI for this representation again yields  $\sqrt{F(s)} \propto 1/s$ , consistent with Weber's law (*Materials and Methods*). Note that unlike the previous case (in which Weber's law arose from the nonlinear transducer), sensitivity in this case arises entirely from the stimulus dependence of the noise variance (Fig. 1B).

Now consider a third case, inspired by neurobiology. Assume the stimulus is internally represented through neural spike counts that are Poisson-distributed with rate  $\mu(s)$  (e.g., refs. 41–43). Despite the discrete nature of the spike count responses, FI may still be computed, and provides a bound on sensitivity. In this case, noise variance is equal to the mean response, and sensitivity is  $\sqrt{F(s)} = |\mu'(s)|/\sqrt{\mu(s)}$ , which gives rise to Weber's law for a transducer function  $\mu(s) \propto [\log(s) + c]^2$ , where  $c$  is an integration constant (Fig. 1C; *Materials and Methods*). Here, sensitivity reflects the combined signal dependence of transducer and noise.

These three different examples demonstrate that an observation of Weber's law sensitivity does not uniquely constrain an internal representation (see also refs. 44–47). In fact, these are three members of an infinite family of representations  $p(r|s)$  whose FI is consistent with Weber's law. To make this nonidentifiability problem more explicit, we introduce a simpler quantity which we dub "Fisher sensitivity", defined as

$$D(s) = \frac{|\mu'(s)|}{\sigma(s)}. \quad [1]$$

In general, Fisher sensitivity provides a lower bound on the square root of FI (48) (*Materials and Methods*), and is easier to compute, since it relies only on the first two moments of the response distribution. Its expression as a ratio of the change in response mean to SD also provides an explicit connection to the d-prime measure used to quantify discriminability in signal detection theory (*Materials and Methods*). For all three of the examples in the preceding paragraphs, this lower bound is exact (i.e., Fisher sensitivity is identical to the square root of FI). But Fisher sensitivity offers a direct and intuitive extension of the nonidentifiability problem beyond these examples: To explain any measured pattern of sensitivity  $D(s)$ , one can choose an arbitrary mean internal response  $\mu(s)$  that increases monotonically and continuously, and pair it with an internal noise with variability  $\sigma(s) = |\mu'(s)|/D(s)$ . How can we resolve this ambiguity?

**Unified Interpretation of Power-Law Intensity Percepts and Weber's Law Sensitivity.** The ambiguity described in the previous section can be resolved through additional measurements (or assumptions) of the mean or variance of internal representations, or the relationship between the two. In this section, we interpret perceptual magnitude ratings as a direct measurement of the representational mean,  $\mu(s)$  (44, 49). In a rating experiment,

observers are asked to report perceived stimulus intensities by selecting a number from a rating scale (e.g., refs. 7, 16, and 17). Suppose that these ratings reflect the observers' internal response  $r$  (up to an arbitrary scale factor that depends on the numerical scale), and that averaging over many trials of  $r$  (drawn from  $p(r|s)$ ) provides an estimate of the mean response,  $\mu(s)$ .

Using magnitude ratings, Stevens and others (e.g., refs. 16, 50, and 51) showed that perceived intensity of many stimulus attributes can be well approximated by a power law,  $\mu(s) \propto s^\alpha$ . The exponent  $\alpha$  was found to vary widely across stimulus attributes ranging from strongly compressive (e.g.,  $\alpha = 0.33$  for brightness of a small visual target) to strongly expansive (e.g.,  $\alpha = 3.5$  for electric shock to fingertips). For stimulus attributes obeying Weber's law, Stevens' power law observations were interpreted as direct evidence against Fechner's hypothesis of logarithmic transducers (11). But the relationship of power law ratings to Weber's law sensitivity was left unresolved. Over the intervening decades, magnitude rating measurements have generally been interpreted as arising from aspects of internal representation that are different from those underlying sensitivity (e.g., refs. 18, 12, 21, and 52), or sometimes, measurements of magnitude ratings were dismissed altogether (9, 13).

Fisher sensitivity offers a potential unification of power-law intensity percepts and Weber's law sensitivity. First, we assume the observer whose discrimination behavior matches Weber's law does so by optimally decoding an internal representation, achieving the Fisher sensitivity:  $D(s) = \frac{|\mu'(s)|}{\sigma(s)} \propto 1/s$ . Substituting a power function,  $\mu(s) = s^\alpha$ , and solving for  $\sigma(s)$  yields (Fig. 2A; *Materials and Methods*):

$$\sigma(s) \propto s^\alpha. \quad [2]$$

Thus, the SD of the internal representation is proportional to its mean. This result holds for all values of  $\alpha$ , and does not assume Gaussian internal noise, thus providing a generalization of the multiplicative noise example from the previous section (Fig. 1). Under these conditions, Weber's law sensitivity can coexist with a power-law intensity percept for any exponent (Fig. 2B).

**Connecting Perceived Intensity and Discrimination of Generalized Intensity Variables.** The previous section provided a unification of three idealized relationships: Weber's law for sensitivity, a power-law behavior for intensity ratings, and proportionality of mean and SD of the internal representation. In this section, we consider generalizations beyond these relationships and show that these can remain consistent under our framework.

Consider first the internal noise. Poisson neural noise implies a variance proportional to the mean spike count, a relationship that holds empirically for relatively low response levels (53). At modest to high firing rates, spike count variance in individual neurons is generally super-Poisson, growing approximately as the square of mean response (53–55), consistent with the proportional noise assumption of the previous section. A modulated Poisson model has variance with both linear and quadratic terms and can capture the relationship of spike count variance to mean response over the extended range (53, 54):

$$\sigma^2(s) = \mu(s) + g^2 \mu^2(s), \quad [3]$$

where the constant  $g$  represents the SD of the modulation, and governs the transition from the Poisson range (smaller  $\mu(s)$ ) to the super-Poisson range (larger  $\mu(s)$ ) (Fig. 3A).

Perceptually, both Weber's law for sensitivity and the power law for perceptual magnitudes are known to fail, especially at low

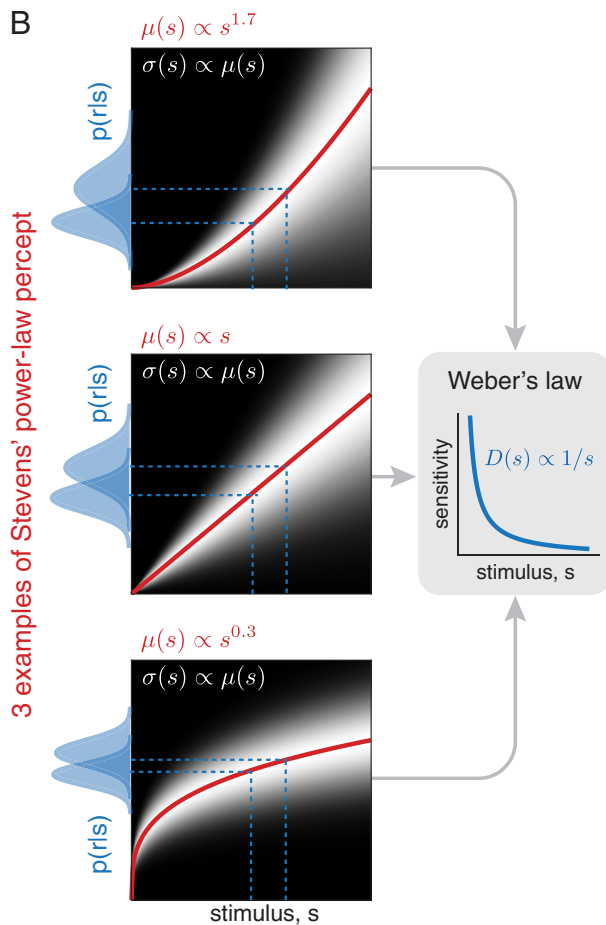
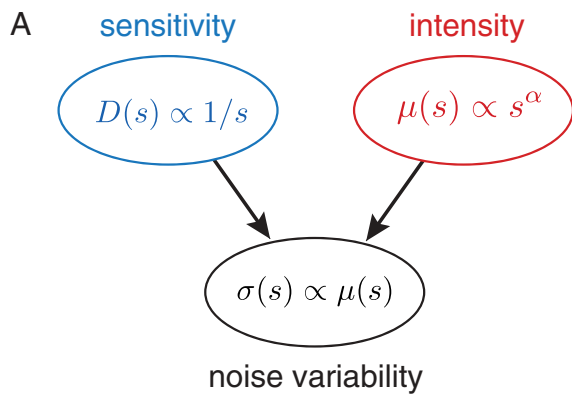


**Fig. 2.** Unification of power-law intensity and Weber's law sensitivity measurements. (A) Using Fisher sensitivity, perceptual sensitivity and intensity measurements can be combined to constrain the noise properties of an internal representation. In the particular case of Weber's law, and power-law intensity ratings, this yields an internal representation with noise SD proportional to mean response. (B) This pattern of proportional internal noise serves to unify Weber's law and power-law magnitudes for any exponent  $\alpha$ , allowing for transducer functions that are expansive ( $\alpha > 1$ , Upper panel), linear ( $\alpha = 1$ , Middle), or compressive ( $\alpha < 1$ , Lower). Blue dashed lines indicate an example pair of stimuli that are equally discriminable in all three cases, as can be deduced qualitatively from the overlap of their corresponding response distributions (shown along the left vertical edge of each plot, in shaded blue).

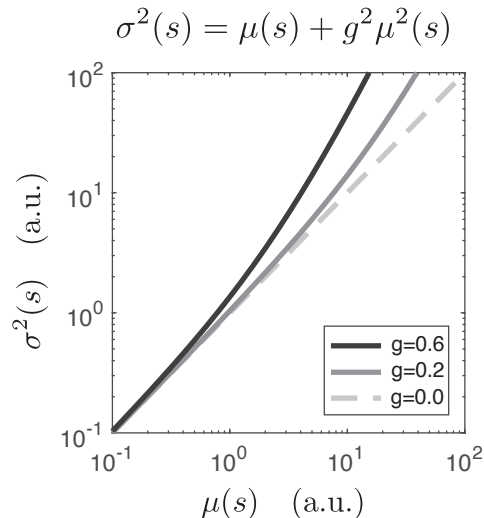
intensities (e.g., refs. 7 and 56). A generalized form of Weber's law (e.g., ref. 57) has been proposed to capture sensitivity data over a broader range of intensity:

$$D(s) = w/(s + d)^\beta, \quad [4]$$

where  $d$  is a constant that governs sensitivity at low intensities, the exponent  $\beta$  determines deviation from Weber's law at high intensities, and  $w$  is a nonnegative scaling factor. Weber's law corresponds to the special case of  $d = 0$  and  $\beta = 1$ .

To test the generalization of our unified framework, we used Fisher sensitivity to combine the modulated Poisson noise model (Eq. 3) with fitted versions of this generalized form of Weber's law (Eq. 4), and to generate predictions of  $\mu(s)$  (Fig. 3B). We then compared these predictions to averaged perceptual intensity ratings. The predictions rely on the choice of three parameters:  $g$  that determines the transition from Poisson to super-Poisson noise, an integration constant  $c$ , and a scale factor that accounts for the range of the rating scale used in the experiment (*Materials and Methods*). We examined predictions for five different stimulus attributes, for which both sensitivity and rating scale data (averaged across trials) are available over

A



B

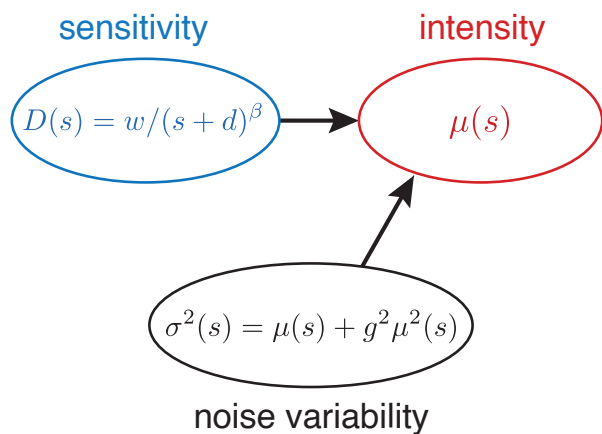


**Fig. 3.** Generalization beyond the Weber range. (A) Quadratic mean-variance relationship for a modulated Poisson model of sensory neurons (53, 55). Behavior is Poisson-like at low intensities [i.e., when  $\mu(s)$  is much less than  $1/g^2$ , then  $\sigma^2(s) \sim \mu(s)$ ], and super-Poisson at higher intensities [when  $\mu(s)$  is much greater than  $1/g^2$ , then  $\sigma^2(s) \sim \mu^2(s)$ ]. (B) Using Fisher sensitivity, a generalized form of Weber sensitivity can be combined with the mean-variance relationship in panel A to generate numerical predictions of perceived stimulus intensity  $\mu(s)$  (see examples in Fig. 4).

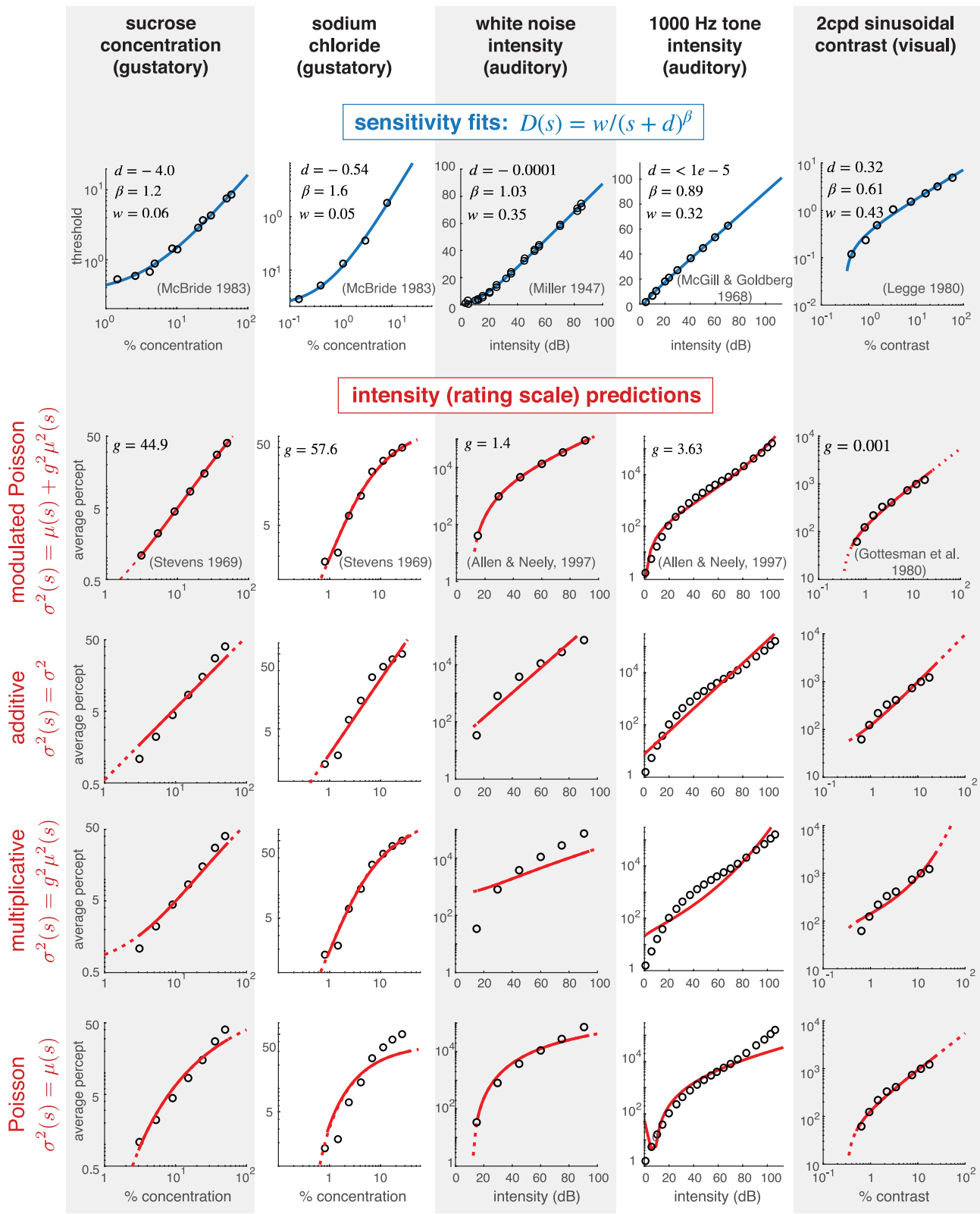


**Fig. 4.** Predictions of perceived intensity from sensitivity, for five different sensory attributes. **Top row:** For each attribute, we fit a three-parameter generalized form of Weber's law (Eq. 4, blue curves) to measured discrimination thresholds (hollow points). Optimal parameter values for each attribute are indicated. **Bottom four rows:** Fitted sensitivity functions are equated to the Fisher sensitivity relationship (Eq. 1) assuming one of four different mean-variance relationships (equations, left side), to generate predictions of perceived intensity  $\mu(s)$  (red curves). The modulated Poisson and multiplicative noise predictions depend on parameter  $g$ , and the additive noise prediction depends on parameter  $\sigma$ . In addition, all predictions depend on an integration constant  $c$  and an overall multiplicative scale factor (Materials and Methods). All parameters are adjusted to best fit average perceptual rating scale measurements (hollow points).

a large range of stimulus intensities. Fig. 4 shows results for: 1) concentration of sucrose [“sweetness” (58, 59)]; 2) concentration of sodium chloride [“saltiness” (58, 59)]; 3) amplitude of white noise [auditory loudness, (60, 61)]; 4) amplitude of 1,000 Hz pure tone [auditory loudness, (61, 62)]; and 5) amplitude of a sinusoidal grating [visual contrast, (51, 57)].

The sensitivity curves vary substantially across these stimulus attributes, but all are well fit by the generalized Weber functional form (blue curves, first row of Fig. 4). In all cases, the rating scale data are well predicted by combining the sensitivity fit with the modulated Poisson noise model of Eq. 3 (red curves, second row, Fig. 4). Moreover, we find that reduction to simpler noise models (multiplicative, or Poisson) that are special cases of the full model provide worse predictions for many cases (rows 4 and 5, Fig. 4). Specifically, when  $g$  is small (as in the case of visual contrast), the modulated Poisson model behaves similarly to a standard Poisson model, but the multiplicative model fit is poor. When  $g$  is large (as in the case of tasting sodium chloride), the noise model behaves similarly to the multiplicative noise model, but the Poisson model fit is poor. Note that the standard Poisson model has one less parameter than the other models.

The additive noise model is also worse than the modulated Poisson model, but generally outperforms the other two (Fig. 4, row 3). In the five stimulus domains examined, we did not observe any systematic pattern of model parameters across stimulus categories (for either the sensitivity fit or the rating scale predictions). But examination of additional stimulus domains using this type of concurrent measurement may reveal such patterns.

## Discussion

Stimulus magnitude and sensitivity are among the most widely assessed perceptual characteristics (63, 64), but the relationship between the two has proven elusive. In this article, we’ve proposed a framework that relates these characteristics to two fundamental properties of internal representation—a nonlinear “transducer” that expresses the mapping of stimulus magnitude to the mean internal representation, and the stimulus-dependent amplitude of internal noise. Our proposal relies on two assumptions that

link perceptual measurements to these properties: 1) sensitivity (the inverse of the discrimination threshold) reflects a combination of the transducer and the noise amplitude, as expressed by Fisher sensitivity; and 2) absolute judgments (specifically, those obtained through average ratings of stimulus intensity) reflect the value of the transducer. This combination allows a unified interpretation in which intensity and sensitivity reflect a single underlying representation, providing a potential link to physiology.

Our framework relies on several assumptions. First, we restrict ourselves to a continuous scalar stimulus domain and an internal representation that is differentiable with respect to the stimulus (so that FI is well defined). Throughout, we rely on Fisher sensitivity, an intuitive and tractable lower bound on the square root of FI. The two are equivalent for the Weber’s law examples shown in Figs. 1 and 2, but not for the data fitting examples of Fig. 4 (in *SI Appendix*, we provide an additional example in which the two quantities differ). We assume human perceptual sensitivity achieves (or is at least proportional to) the Fisher sensitivity bound. More specifically, we assume that human responses in a perceptual discrimination task reflect optimal extraction of information from a noisy internal representation, as suggested by a number of studies linking physiology to perception (e.g., refs. 65–69). Finally, we assume that absolute intensity judgments reflect a transducer function that corresponds to the mean of the internal representation.

To develop and test this framework, we have focused on attributes that obey Weber’s law, and its modest generalizations. Despite its ubiquity, the relationship between Weber’s law and the underlying representation has been contentious. In the late 19th century, Fechner proposed that perceptual intensities correspond to integrated sensitivity (1), and, in particular, predicted that Weber’s law sensitivity implied a logarithmic internal representation. Using rating scales as a form of measurement, Stevens instead reported that many sensory variables appeared to obey a power law, with exponents differing substantially for different attributes (11). Stevens interpreted this as a refutation of Fechner’s logarithmic transducer. In order to explain the discrepancy between Fechner and Stevens’ proposals, a number of authors suggest that perceptual intensities and sensitivity reflect

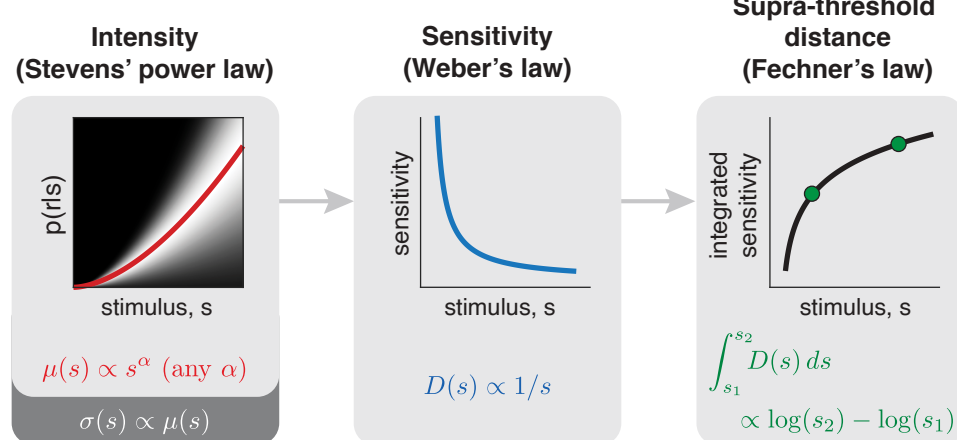


**Fig. 5.** Extension of the Fisher sensitivity framework to suprathreshold perceptual distances. Weber’s law is consistent with Stevens’ power law (for any exponent,  $\alpha$ ) as long as the SD of the noise scales with the same exponent (Left and Middle panels; see also Fig. 2B). In addition, under the assumption that perceived suprathreshold distances correspond to *integrated* sensitivity, these will correspond to differences in logarithmically mapped stimuli, providing a modified interpretation of Fechner’s law. Under these conditions, all three “laws” coexist in a consistent framework, each describing measurements that access different aspects of a common underlying representation.

different stages of processing, bridged by an additional nonlinear transform. Specifically, Michels and Helson (18) proposes a type of sensory adaptation, Mackay (19) reflects additional sensory processing, and Krueger (22) incorporates an additional cognitive process. Our framework offers a parsimonious resolution of these discrepancies, by postulating that perceptual intensity and sensitivity arise from different combinations of the mean and variance of a common internal representation.

It is worth noting that while Fechner's integration hypothesis is inconsistent with Stevens' power law measurements, it appears to be consistent with many suprathreshold intensity measurements. Specifically, experimental procedures involving suprathreshold comparative judgments [e.g., maximum likelihood difference scaling methods, categorical scales, and bisection procedures (17, 40, 58, 70)] seem to reflect integration of sensitivity, whereas experimental procedures that require absolute judgments [e.g., rating scales (17, 51, 71)] yield different functions that we've interpreted as reflecting the mean of internal representation. In the case of Weber's law, the integrated sensitivity is logarithmic, consistent with Fechner's interpretations, regardless of the underlying transducer-noise combination (e.g., Fig. 1)! Under this interpretation, our framework can provide a natural unification of Stevens' power law magnitude ratings, Weber's law sensitivity, and Fechner's logarithmic suprathreshold distances (Fig. 5). Further empirical studies will be needed to verify or refute these relationships.

This subtle distinction between comparative and absolute judgment is at the heart of multiple debates in perceptual literature. For example, it arises in discussions of whether perceptual noise is additive or multiplicative in visual contrast (e.g., refs. 40, 44, and 72). We have proposed that mean and variance of internal representations can be identified through the combination of absolute and discriminative judgments, because the two measurements reflect different aspects of the representation. On the other hand, if suprathreshold comparative judgments reflect integrated local sensitivity, they will not provide additional constraints on internal representation beyond threshold sensitivity measurements, and combining these two measurements cannot resolve the identifiability issue. This provides, for example, a consistent interpretation of the analysis in ref. 40, which shares the logic of our approach in seeking an additional measurement to resolve nonidentifiability of sensitivity measurements, but reaches a different conclusion regarding consistency of additive noise. Several other theoretical or experimental constraints have been proposed to resolve the identifiability issue, including imposing a common criterion between two discrimination tasks (72), connecting the response accuracy for the first and the second response in a four-alternative choice (31), and connecting discrimination to an identification task (47). An open question is whether our framework can be extended to account for these more diverse perceptual scenarios.

Our examination of the particular combination of Weber's law sensitivity with power-law intensity percepts led to the conclusion that the SD of internal noise in these cases should vary in proportion to the mean response. While such "multiplicative noise" has been previously proposed as an explanation for Weber's law (3, 35–37), it has generally been described in the context of a linear transducer (as in Fig. 1). In our framework, we find that this form of noise (SD proportional to the mean) is sufficient to unify Weber's and Stevens' observations for the complete family of power-law transducers, regardless of exponent. An additional prediction of this model is that the SD of perceptual magnitude

ratings should grow proportionally to the mean rating (consistent with Fig. 2B). This is consistent with the findings of a number of previous studies (e.g., refs. 10, 73, and 74). For example, Green and Luce showed that when observers were asked to rate 1,000 Hz tone loudness, their coefficient of variations (SD divided by the mean) in the ratings are near-constant for a wide range of intensities (73).

The proportionality of the mean and SD of a stimulus representation offers a potential interpretation in terms of underlying physiology of neural responses. We considered, in particular, recently proposed "modulated Poisson" models for neural response which yields noise whose variance grows as a second-order polynomial of the mean response (53, 54, 75). At high levels of response, this allows a unification of Weber's law and Stevens' power law. At lower levels, it produces systematic deviations that lead to consistent predictions of ratings for a number of examples (Fig. 4). Recent generalizations of the modulated Poisson model may allow further refinement of the perceptual predictions (76). For example, at very low levels of response, sensory neurons exhibit spontaneous levels of activity that are independent of stimulus drive (34), suggesting that inclusion of an additive constant in Eq. 3 could improve predictions of perceptual detection thresholds (77).

We've restricted our examples to perceptual intensity attributes that obey Weber's law, but the proposed framework is more general. In particular, the FI bound holds for any noisy representation, and has, for example, been applied to the representation of sensory variables in neural population responses (e.g., 25, 28, 29). In some cases, these attributes exhibit Weber's law behavior, which may be ascribed to the combination of heterogeneous arrangements of neural tuning curves along with noise properties of individual neurons (78–80). For example, neurons in visual area MT selective for different speeds have tuning curves that are (approximately) shifted on a logarithmic speed axis (81). Under these conditions, an independent response noise model yields FI consistent with Weber's law (82, 83). More generally, changes in a stimulus attribute may cause changes in both the amplitude and the pattern of neuronal responses, which, when coupled with properties of internal noise, yield predictions of sensitivity through FI. Specifically, the abstract internal representation that we have assumed for each perceptual attribute corresponds to the projection of high-dimensional noisy neuronal responses onto a decision axis for perceptual judgments (e.g., refs. 54, 84, and 85). Although discrimination judgments for a stimulus attribute are generally insufficient to uniquely constrain underlying high-dimensional neuronal responses, the one-dimensional projection of these responses provides an abstract but useful form for unifying the perceptual measurements.

Our framework enables the unification of two fundamental forms of perceptual measurement—magnitude judgment and sensitivity—with respect to a common internal representation. However, the study of perception is diverse and mature, with numerous additional perceptual measurements (86) whose connection to this framework could be explored. The descriptive framework outlined here also raises fundamental questions about the relationship between internal representation mean and noise. The forms of both noise and transducer may well be constrained by their construction from biological elements, but may also be coadapted to satisfy normative goals of efficient transmission of environmental information under constraints of finite coding resources (87–89). Exploration of these relationships provides an enticing direction for future investigation.

## Materials and Methods

**Fisher Information.** For a stimulus attribute  $s$ , the FI is derived from the conditional distribution of responses given the stimulus,  $p(r|s)$ , and expresses the relative change in response distribution when the stimulus  $s$  is perturbed:

$$F(s) = \mathbb{E}\left[(\partial \log p(r|s)/\partial s)^2\right], \quad [5]$$

where the expectation is taken over the distribution  $p(r|s)$  (90). Intuitively, FI converts a description of the internal noisy representation,  $p(r|s)$ , into a measure of the precision (inverse variance) with which the stimulus is represented (91). The definition relies only on the differentiability of the response distribution with respect to  $s$  and some modest regularity conditions (91), but does not make assumptions regarding the form of the noisy response distribution. Either  $s$  or  $r$  can be vector-valued, but for our purposes in this article, we assume a one-dimensional stimulus attribute, and thus the internal representation  $r$  that is relevant to the discrimination experiment is also effectively one-dimensional.

In statistics and engineering communities, FI is often used in the context of the Cramér–Rao bound, an upper bound on the precision (inverse variance) attainable by an unbiased estimator (91). It was first proposed as a means of quantifying perceptual discrimination by Paradiso (29), and further elaborated for neural populations by Seung and Sompolinsky (25). In this context, the square root of FI provides a bound on perceptual precision (sensitivity) (30), and may be viewed as a generalization of d-prime (27), the traditional metric of signal detection used in psychophysical studies (3) (*SI Appendix*).

**Three Example Representations Yielding Weber’s Law Sensitivity.** The three example representations shown in Fig. 1 are each consistent with Weber’s law, but differ markedly in their response distributions. Below, we derive each of these.

**Additive Gaussian noise.** Assume the internal representation has mean response  $\mu(s)$ , and is contaminated with additive Gaussian noise with SD  $\sigma$ :

$$p(r|s) = (\sqrt{2\pi}\sigma)^{-1} \exp[-(r - \mu(s))^2/(2\sigma^2)].$$

Substituting into Eq. 5 and simplifying yields  $\sqrt{F(s)} = |\mu'(s)|/\sigma$ . Weber’s law corresponds to sensitivity proportional to  $1/s$ , and thus we require a transducer such that  $|\mu'(s)| \propto 1/s$ . If we assume monotonicity, the transducer is uniquely determined (up to an integration constant and a proportionality factor) via integration:  $\mu(s) \propto \log(s) + c$ .

**“Multiplicative” Gaussian noise.** Assume a representation with identity transducer  $\mu(s) = s$  and Gaussian noise such that the amplitude scales with the mean,  $\sigma(s) = \sqrt{as}$ :

$$p(r|s) = (\sqrt{2\pi}as)^{-1} \exp[-(r - \mu(s))^2/(2as^2)].$$

Substituting into Eq. 5 and simplifying again yields Weber’s law:  $\sqrt{F(s)} = (\sqrt{2+1/a}s)$ .

**Poisson noise.** Assume the internal response  $r$  is an (integer) spike count, drawn from an inhomogeneous Poisson process with rate  $\mu(s)$ , a widely used statistical description of neuronal spiking variability. Then

$$p(r|s) = \frac{\mu(s)^r \exp[-\mu(s)]}{r!}.$$

In this case,  $\sqrt{F(s)} = |\mu'(s)|/\sqrt{\mu(s)}$ . Assuming Weber’s law, we can again derive the form of the transducer:  $\mu(s) \propto [\log(s) + c]^2$  for some constant  $c$ .

**Fisher Sensitivity.** In general, FI can be difficult to compute and often cannot be expressed in closed form. A lower bound for the square root of FI, which we term “Fisher sensitivity”, is more easily computed and interpreted, because it depends only on the mean and variance of the distribution. Specifically, we define Fisher sensitivity as

$$D(s) \equiv |\mu'(s)|/\sigma(s).$$

Its role as a lower bound can be derived using the Cauchy–Schwartz inequality for continuous density  $p(x)dx$ :

$$\int f(x)^2 p(x) dx \geq \frac{\left[\int g(x)f(x)p(x) dx\right]^2}{\int g(x)^2 p(x) dx}. \quad [6]$$

Making the following substitutions:

$$f(x) \rightarrow \frac{\partial \log p(r|s)}{\partial s}, \quad g(x) \rightarrow r - \mu(s), \quad p(x)dx \rightarrow p(r|s)dr, \quad [7]$$

the left side of Eq. 6 is equal to the FI (defined in Eq. 5), and the right side is equal to the squared Fisher sensitivity:

$$\begin{aligned} F(s) &\geq \frac{\left\{\int [r - \mu(s)] \frac{\partial \log p(r|s)}{\partial s} p(r|s) dr\right\}^2}{\int [r - \mu(s)]^2 p(r|s) dr} \\ &= \frac{\left\{\int [r - \mu(s)] \frac{\partial p(r|s)}{\partial s} dr\right\}^2}{\sigma(s)^2} \\ &= \frac{\left\{\frac{\partial}{\partial s} \int rp(r|s) dr - \mu(s) \frac{\partial}{\partial s} \int p(r|s) dr\right\}^2}{\sigma(s)^2} \\ &= \frac{\mu'(s)^2}{\sigma(s)^2} \\ &= D^2(s). \end{aligned} \quad [8]$$

Fishersensitivity generalizes to multidimensional response vectors (e.g., a neural population), by replacing the inverse variance with the FI matrix, and projecting this onto the gradient of the mean response (92, 93). The derivation of the full bound for the multidimensional case (both stimuli and responses) may be found in ref. (48).

In the examples of Figs. 1 and 2, the lower bound is exact: Fisher sensitivity is equal to the square root of FI. An equivalent expression for Fisher sensitivity has also been derived by assuming a minimal-variance unbiased linear decoder (94). Compared to our interpretation as a lower bound, this interpretation has the advantage of being an exact expression of FI, but the disadvantage of relying on restrictive decoding assumptions.

**Relationship of Fisher Sensitivity to Signal Detection Theory.** In signal detection theory, discriminability between two stimulus levels  $s_1$  and  $s_2$  is typically summarized using the measure known as d-prime. To relate this to Fisher sensitivity, we assume a simple form sometimes used in the perception literature:

$$d'(s_1, s_2) = \frac{\mu(s_2) - \mu(s_1)}{\sigma(\bar{s})}, \quad \text{with } \bar{s} = \frac{s_1 + s_2}{2}. \quad [9]$$

Assuming  $s_1$  and  $s_2$  are two values on a continuum, and that  $\mu(s)$  is differentiable, we can express the two internal responses using a first-order (linear) Taylor approximation:

$$\mu(s_1) \approx \mu(\bar{s}) + (s_1 - \bar{s})\mu'(\bar{s}), \quad \mu(s_2) \approx \mu(\bar{s}) + (s_2 - \bar{s})\mu'(\bar{s}).$$

Substituting these into Eq. 9 gives

$$\begin{aligned} d'(s_1, s_2) &\approx \frac{\Delta s \mu'(\bar{s})}{\sigma(\bar{s})}, \quad \text{with } \Delta s = s_2 - s_1, \\ &= \Delta s D(\bar{s}). \end{aligned} \quad [10]$$

That is, Fisher sensitivity expresses the slope at which d-prime increases with stimulus separation [see also (27)]. Setting d-prime equal to a criterion level  $d^*$  and solving for the stimulus discrimination threshold gives

$$\Delta s \approx d^*/D(\bar{s}).$$

That is, discrimination thresholds are inversely proportional to Fisher sensitivity. This relationship was used to fit the data for Fig. 4.

**Internal Representations Consistent with Weber's Law and Stevens' Power Law.** Using Fisher sensitivity and assuming monotonicity of  $\mu(s)$ , Weber's law can be expressed as  $\frac{\mu'(s)}{\sigma(s)} \propto \frac{1}{s}$ . To identify  $\mu(s)$  and  $\sigma(s)$ , we combine this with magnitude ratings, which we assume provide a direct measurement of  $\mu(s)$ . Assume the magnitude ratings follow a power law (16). Then  $\mu(s) \propto s^\alpha$ , with derivative  $\mu'(s) = \alpha s^{\alpha-1}$ . Substituting into the equation for Weber's law and solving gives  $\sigma(s) \propto s^\alpha$ . That is, Weber's law can arise when both  $\mu(s)$  and  $\sigma(s)$  follow a power law with the same exponent,  $\alpha$ . Note that this result holds for all exponents.

**Data Fitting.** To examine the validity of our framework beyond Weber's range, we analyzed five different sensory attributes (Fig. 4). For each, we first fit a generalized form of Weber's law (20) to perceptual sensitivity data:

$$D(s) = \frac{w}{(s-d)^\beta}, \quad [11]$$

in which  $d$  is an unrestricted additive constant,  $\beta$  is a nonnegative exponent, and  $w$  is a nonnegative scaling factor. These three parameters were optimized to minimize squared error of the measured thresholds (inverse sensitivity).

Next, we combined the fitted sensitivity model with a model of internal noise to generate a prediction for the mean percept,  $\mu(s)$ , which was then compared with rating measurements. This was carried out for four different noise models: modulated Poisson, additive, multiplicative, and Poisson (corresponding to the bottom four rows of Fig. 4, respectively). We derive the corresponding expressions for  $\mu(s)$  below.

**Modulated Poisson noise.** Our primary predictions assume a modulated Poisson noise model (53) with mean-variance relationship:

$$\sigma(s)^2 = \mu(s) + g^2 \mu(s)^2. \quad [12]$$

The transducer  $\mu(s)$  is obtained by solving the differential equation that arises by substituting this variance expression into the Fisher sensitivity of Eq. 1, and equating this with the generalized form of Weber's law (Eq. 11):

$$\frac{\mu'(s)}{\sqrt{\mu(s) + g^2 \mu(s)^2}} = \frac{w}{(s-d)^\beta}. \quad [13]$$

The solution may be expressed in closed form:

$$\mu(s) = \sinh^2 \left( \frac{g(s-d)^{-\beta} [w(d-s) + c(s-d)^\beta]}{2(\beta-1)} \right) / g^2. \quad [14]$$

The parameters  $\{d, \beta, w\}$  are constrained to values obtained when fitting the sensitivity data, and three remaining parameters are adjusted to minimize squared error with the log-transformed rating data. The first is  $g$ , which governs the transition from Poisson to super-Poisson noise behavior (large  $g$  indicates an early transition). The second is  $c$ , an integration constant that arises from solving the differential equation for  $\mu(s)$ . The last parameter is an overall scale factor

(not indicated), which rescales the predicted intensity values to the numerical range used in the associated rating experiment.

**Additive Gaussian noise.** As for the full modulated Poisson model, we first fit the generalized Weber's law to discrimination data, and locked the parameters  $\{d, \beta, w\}$ . Then we solve a differential equation arising from equating Fisher sensitivity with the generalized Weber's law:

$$\frac{\mu'(s)}{\sigma} = \frac{w}{(s-d)^\beta}. \quad [15]$$

The solution for  $\mu(s)$  in this case may also be expressed in closed form:

$$\mu(s) = \frac{w\sigma(s-d)^{1-\beta}}{1-\beta} + c. \quad [16]$$

The integration constant  $c$ , the constant  $\sigma$ , and an overall scaling factor are adjusted to fit  $\mu(s)$  to the rating data (minimizing the squared error between logarithmically transformed rating data and the function).

**Poisson noise.** Following a similar procedure for the case of additive Gaussian noise, we find a closed-form solution for  $\mu(s)$  using Poisson noise and Fisher sensitivity:

$$\mu(s) = \frac{(s-d)^{-2\beta} [w(d-s) + (\beta-1)c(s-d)^\beta]^2}{4(\beta-1)^2}. \quad [17]$$

Again, the integration constant  $c$  and overall scaling factor are optimized to fit the rating data.

**Generalized multiplicative noise.** Here, we assume a noise mean-variance relationship  $\sigma(s)^2 = g^2 \mu(s)^2$ , which is the choice that enables the coexistence of the classic form of Weber's law and Stevens' power law. As in previous cases, we substitute this into the expression for Fisher sensitivity to obtain a prediction for  $\mu(s)$ :

$$\mu(s) = \exp \left[ \frac{gw(s-d)^{(1-\beta)}}{1-\beta} \right] c. \quad [18]$$

Note that, as for the full noise model of Eq. 12, comparison to the rating data involves estimation of three parameters: the noise parameter  $g$ , an integration constant  $c$ , and a scaling factor.

**Data, Materials, and Software Availability.** All study data are included in the article and/or [SI Appendix](#). Simulations and code for fitting the data can be found at [https://github.com/JingyZhou1/weberStevens\\_code\\_data](https://github.com/JingyZhou1/weberStevens_code_data) (95).

**ACKNOWLEDGMENTS.** We thank Nikhil Parthasarathy, Mike Landy, Tony Movshon, David Brainard, Robbe Goris, Bill Geisler, Larry Maloney, Jacob Cheeseman, and members of the Center for Computational Neuroscience at the Flatiron Institute for helpful discussions and suggestions. In addition, we are grateful to the editor and three reviewers for their constructive questions and suggestions, which encouraged a variety of improvements in the manuscript.

1. G. Fechner, *Elemente der Psychophysik* (Breitkopf and Hartel, Leipzig, Germany, 1860).
2. W. P. Tanner, J. A. Swets, A decision-making theory of visual detection. *Psychol. Rev.* **61** (6), 401–409 (1954).
3. D. Green, J. Swets, *Signal Detection Theory and Psychophysics* (Robert E. Krieger Publishing Company, 1966).
4. J. A. F. Plateau, Sur la mesure des sensations physiques, et sur la loi qui lie l'intensité de ces sensations l'intensité de la cause excitante (1872).
5. L. Thurstone, Fechner's law and the method of equal-appearing intervals. *J. Exp. Psychol.* **12**, 214–224 (1929).
6. E. Newman, J. Volkmann, S. Stevens, On the method of bisection and its relation to a loudness scale. *Am. J. Psychol.* **49**, 134–137 (1937).
7. S. Stevens, *Psychophysics: Introduction to Its Perceptual, Neural, and Social Prospects* (John Wiley and Sons Inc., New York, NY, 1975).
8. C. Kopec, C. Brody, Human performance on the temporal bisection task. *Brain Cogn.* **74**, 262–72 (2010).
9. S. Prytulak, Critique of S.S. Stevens' theory of measurement scale classification. *Percept. Motor Skills* **41**, 3–28 (1975).
10. F. H. Petzschner, S. Glasauer, S. K. E., A Bayesian perspective on magnitude estimation. *Trends Cognit. Sci.* **19**, 285–293 (2015).
11. S. Stevens, To honor Fechner and repeal his law: A power function, not a log function, describes the operating characteristic of a sensory system. *Science* **133**, 80–86 (1961).
12. W. Wagenaar, Stevens vs. Fechner—Plea for dismissal of case. *Acta Psychol.* **39**, 225–235 (1975).
13. D. Weiss, The impossible dream of Fechner and Stevens. *Perception* **10**, 431–434 (1981).
14. D. Murray, A perspective for viewing the history of psychophysics. *Behav. Brain Sci.* **16**, 115–137 (1993).
15. R. Shapley, C. Enroth-Cugell, Visual adaptation and retinal gain control. *Progr. Retinal Res.* **3**, 263–346 (1984).
16. S. Stevens, On the psychophysical law. *Psychol. Rev.* **64**, 153–181 (1957).
17. S. Stevens, E. Galanter, Ratio scales and category scales for a dozen perceptual continua. *J. Exp. Psychol.* **54**, 377–411 (1957).
18. W. Michels, H. Helson, A reformulation of the Fechner law in terms of adaptation-level applied to rating-scale data. *Am. J. Psychol.* **62**, 355–368 (1949).
19. D. Mackay, Psychophysics of perceived intensity—A theoretical basis for Fechners and Stevens laws. *Science* **139**, 1213–1214 (1963).
20. M. Treisman, Sensor scaling and the psychophysical law. *Q. J. Exp. Psychol.* **16**, 11–22 (1964).
21. M. Copelli, A. Roque, R. Oliveira, O. Kinouchi, Physics of psychophysics: Stevens and Weber-Fechner laws are transfer functions of excitable media. *Phys. Rev. E Stat. Nonlinear Soft Matter Phys.* **65**, 060901 (2002).

22. L. Krueger, Reconciling Fechner and Stevens: Toward a unified psychophysical law. *Behav. Brain Sci.* **12**, 251 (1989).
23. A. Nieder, E. K. Miller, Coding of cognitive magnitude: Compressed scaling of numerical information in the primate prefrontal cortex. *Neuron* **37**, 149–157 (2003).
24. D. G. Pelli, Uncertainty explains many aspects of visual contrast detection and discrimination. *J. Opt. Soc. Am. A* **2**, 1508–1532 (1985).
25. H. Seung, H. Sompolinsky, Simple models for reading neuronal population codes. *Proc. Natl. Acad. Sci. U.S.A.* **90**, 10749–10753 (1993).
26. L. Itti, J. Braun, D. Lee, C. Koch, A model of early visual processing. *Adv. Neural Inf. Process. Syst.* **10**, 173–179 (1997).
27. N. Brunel, J. P. Nadal, Mutual information, Fisher information, and population coding. *Neural Comput.* **10**, 1731–1757 (1998).
28. B. B. Averbeck, D. Lee, Effects of noise correlations on information encoding and decoding. *J. Neurophysiol.* **95**, 3633–3644 (2006).
29. M. A. Paradiso, A theory for the use of visual orientation information which exploits the columnar structure of striate cortex. *Biol. Cybernet.* **58**, 35–49 (1988).
30. P. Series, A. Stocker, E. P. Simoncelli, Is the homunculus aware of sensory adaptation? *Neural Comput.* **21**, 3271–3304 (2009).
31. A. J. Solomon, Intrinsic uncertainty explains second responses. *Spat. Vis.* **20**, 45–60 (2007).
32. A. Berardino, V. Laparra, J. Ball, E. P. Simoncelli, "Eigen-distortions of hierarchical representations" in *Adv. Neural Inf. Process. Syst. (NIPS\*17)*, I. Guyon *et al.*, Eds. (Curran Associates, Inc., 2017), vol. 30, pp. 3530–3539.
33. L. L. Thurstone, Psychophysical analysis. *Am. J. Psychol.* **38**, 368–389 (1927).
34. W. Geisler, *Ideal Observer Analysis* (MIT Press, 2002).
35. W. P. Tanner, Application of the theory of signal detectability to amplitude discrimination. *J. Acoust. Soc. Am.* **33**, 1233–1244 (1961).
36. G. Werner, V. B. Mountcastle, Neural activity in mechanoreceptive afferents: Stimulus-response relations, Weber functions and information transmission. *J. Neurophysiol.* **28**, 359–397 (1965).
37. W. O. Siebert, Some implications of the stochastic behaviour of primary auditory neurons. *Kybernetik* **2**, 206–214 (1965).
38. E. Eijkman, J. M. Thijssen, J. H. Vendrik, Weber's law, power law, and internal noise. *J. Acoust. Soc. Am.* **40**, 1164–1173 (1966).
39. M. Wojtczak, N. Viemeister, Perception of suprathreshold amplitude modulation and intensity increments: Weber's law revisited. *J. Acoust. Soc. Am.* **123**, 2220–2236 (2008).
40. F. Kingdom, Fixed versus variable internal noise in contrast transduction: The significance of Whittle's data. *Vis. Res.* **128**, 1–5 (2016).
41. A. F. Dean, The variability of discharge of simple cells in the cat striate cortex. *Exp. Brain Res.* **44**, 437–440 (1981).
42. D. J. Tolhurst, J. A. Movshon, A. F. Dean, The statistical reliability of single neurons in cat and monkey visual cortex. *Vis. Res.* **23**, 775–785 (1983).
43. W. R. Softky, C. Koch, The highly irregular firing of cortical cells is inconsistent with temporal integration of random epsps. *J. Neurosci.* **13**, 334–350 (1993).
44. L. Kontsevich, C. Chen, C. Tyler, Separating the effects of response nonlinearity and internal noise psychophysically. *Vis. Res.* **42**, 1771–1784 (2002).
45. M. García-Pérez, R. Alcalá-Quintana, Fixed vs. variable noise in 2AFC contrast discrimination. *Spat. Vis.* **22**, 273–300 (2009).
46. M. Katkov, M. Tsodyks, D. Sagi, Singularities in the inverse modeling of 2AFC contrast discrimination data. *Vis. Res.* **46**, 259–266 (2006).
47. M. Katkov, M. Tsodyks, D. Sagi, Inverse modeling of human contrast response. *Vis. Res.* **47**, 2855–2867 (2007).
48. M. Stein, A. Mezghani, J. Nossek, A lower bound for the fisher information measure. *IEEE Signal Process. Lett.* **21**, 796–799 (2014).
49. V. Mountcastle, G. Poggio, G. Werner, The relation of thalamic cell response to peripheral stimuli varied over an intensive continuum. *J. Neurophysiol.* **26**, 807–834 (1963).
50. J. Stevens, E. Tulving, Estimations of loudness by a group of untrained observers. *Am. J. Psychol.* **70**, 600–605 (1957).
51. J. Gottesman, G. Rubin, G. Legge, A power law for perceived contrast in human vision. *Vis. Res.* **21**, 791–799 (1981).
52. V. Billotck, B. Tsou, To honor Fechner and obey Stevens: Relationships between psychophysical and neural nonlinearities. *Psychol. Bull.* **137**, 1–18 (2011).
53. R. Goris, J. Movshon, E. Simoncelli, Partitioning neuronal variability. *Nat. Neurosci.* **17**, 858–865 (2014).
54. A. K. Churchland *et al.*, Variance as a signature of neural computations during decision-making. *Neuron* **69**, 818–831 (2014).
55. I. Lin, M. Okun, M. Carandini, K. Harris, The nature of shared cortical variability. *Neuron* **87**, 644–656 (2015).
56. W. A. Yost, *Fundamentals of Hearing: An Introduction* (Emerald Group Publishing Limited, 2006).
57. G. Legge, A power-law for contrast discrimination. *Vis. Res.* **21**, 457–467 (1980).
58. R. McBride, A JND-scale/category-scale convergence in taste. *Percept. Psychophys.* **34**, 77–83 (1983).
59. S. Stevens, Sensory scales of taste intensity. *Percept. Psychophys.* **6**, 302–308 (1969).
60. G. Miller, Sensitivity to changes in the intensity of white noise and its relation to masking and loudness. *J. Acoust. Soc. Am.* **19**, 609–619 (1947).
61. J. Allen, S. Neely, Modeling the relation between the intensity just-noticeable difference and loudness for pure tones and wideband noise. *J. Acoust. Soc. Am.* **102**, 3628–3646 (1997).
62. W. McGill, J. Goldberg, Pure-tone intensity discrimination as energy detection. *J. Acoust. Soc. Am.* **19**, 609–619 (1968).
63. R. W. Fleming, Material perception. *Annu. Rev. Vis. Sci.* **3**, 365–88 (2017).
64. L. T. Maloney, K. Knoblauch, Measuring and modeling visual appearance. *Annu. Rev. Vis. Sci.* **6**, 519–537 (2020).
65. F. Rieke, D. A. Baylor, Single-photon detection by rod cells of the retina. *Rev. Mod. Phys.* **70**, 1027–1036 (1998).
66. H. B. Barlow, Critical limiting factors in the design of the eye and visual cortex. *Proc. R. Soc. Lond. B* **212**, 1–34 (1981).
67. K. H. Britten, M. N. Shadlen, W. T. Newsome, J. A. Movshon, The analysis of visual motion: A comparison of neuronal and psychophysical performance. *J. Neurosci.* **12**, 4745–4765 (1992).
68. C. Harris, D. Wolpert, Signal-dependent noise determines motor planning. *Nature* **394**, 780–784 (1998).
69. L. C. Osborne, S. G. Lisberger, W. Bialek, A sensory source for motor variation. *Nature* **437**, 412–416 (2005).
70. A. E. O. Munsell, L. L. Sloan, I. H. Godlove, Neutral value scales. I. Munsell neutral value scale. *J. Opt. Soc. Am.* **23**, 394–411 (1933).
71. S. Stevens, The psychophysics of sensory function. *Am. Sci.* **48**, 226–253 (1960).
72. A. Gorea, D. Sagi, Disentangling signal from noise in visual contrast discrimination. *Nat. Neurosci.* **4**, 1146–1150 (2001).
73. D. Green, R. D. Luce, Variability of magnitude estimates: A timing theory analysis. *Percept. Psychophys.* **15**, 291–300 (1974).
74. J. Gibbon, Scalar expectancy theory and Weber's law in animal timing. *Psychol. Rev.* **84**, 279–325 (1977).
75. K. May, J. Solomon, Connecting psychophysical performance to neuronal response properties. I: Discrimination of suprathreshold stimuli. *J. Vis.* **15**, 8 (2015).
76. A. S. Charles, J. W. Pillow, Dethroning the fano factor: A flexible, model-based approach to partitioning neural variability. *Neural Comput.* **30**, 1012–1045 (2018).
77. P. M. Bays, A signature of neural coding at human perceptual limits. *J. Vis.* **16**, 1–12 (2016).
78. D. Ganguli, E. P. Simoncelli, "Implicit encoding of prior probabilities in optimal neural populations" in *Adv. Neural Inf. Process. Syst. (NIPS\*10)*, J. Lafferty *et al.*, Eds. (MIT Press, 2010), vol. 23, pp. 658–666.
79. B. J. Fischer, J. L. Pena, Owl's behavior and neural representation predicted by Bayesian inference. *Nat. Neurosci.* **28**, 1061–1066 (2011).
80. A. R. Girshick, M. S. Landy, E. P. Simoncelli, Cardinal rules: Visual orientation perception reflects knowledge of environmental statistics. *Nat. Neurosci.* **5**, 926–932 (2011).
81. H. Nover, C. H. Anderson, G. C. DeAngelis, A logarithmic, scale-invariant representation of speed in macaque middle temporal area accounts for speed discrimination performance. *J. Neurosci.* **25**, 10049–10069 (2005).
82. A. A. Stocker, E. P. Simoncelli, Noise characteristics and prior expectations in human visual speed perception. *Nat. Neurosci.* **9**, 578–585 (2006).
83. L. Q. Zhang, A. A. Stocker, Prior expectations in visual speed perception predict encoding characteristics of neurons in area MT. *J. Neurosci.* **42**, 2951–2962 (2022).
84. I. Kanitscheider, R. Coen-Cagli, A. Pouget, Origin of information-limiting noise correlations. *Proc. Natl. Acad. Sci. U.S.A.* **112**, E6973–E6982 (2015).
85. J. Beck, V. R. Bejjanki, A. Pouget, Insights from a simple expression for linear fisher information in a recurrently connected population of spiking neurons. *Neural Comput.* **23**, 1484–1502 (2011).
86. F. A. A. Kingdom, N. Prins, *Psychophysics* (Elsevier Science, 2009).
87. H. B. Barlow, Possible principles underlying the transformation of sensory message. *Sensory Commun.*, 217–234 (1961).
88. D. Ganguli, E. Simoncelli, Efficient sensory encoding and Bayesian inference with heterogeneous neural populations. *Neural Comput.* **26**, 2103–2134 (2014).
89. X. Wei, A. Stocker, Lawful relation between perceptual bias and discriminability. *Proc. Natl. Acad. Sci. U.S.A.* **114**, 10244–10249 (2017).
90. R. A. Fisher, On the mathematical foundations of theoretical statistics. *Philos. Trans. R. Soc. London* **222**, 309–368 (1922).
91. S. M. Kay, *Fundamentals of Statistical Signal Processing—Estimation Theory* (Pearson Education, Inc., 1993).
92. R. Moreno-Bote *et al.*, Information-limiting correlations. *Nat. Neurosci.* **17**, 1410–1417 (2014).
93. J. Malo *et al.*, Estimating the contribution of early and late noise in vision from psychophysical data, arXiv [Preprint] (2024). <https://doi.org/10.48550/arXiv.2012.06608> (Accessed 14 May 2024).
94. M. Kfashan *et al.*, Scaling of sensory information in large neural populations shows signatures of information-limiting correlations. *Nat. Commun.* **12**, 473 (2021).
95. J. Zhou, weberStevens\_code\_data. [https://github.com/JingyZhou1/weberStevens\\_code\\_data](https://github.com/JingyZhou1/weberStevens_code_data). Accessed 15 October 2025.